DOI: 10.1002/cphc.201200048

Intracrystalline Diffusion in Mesoporous Zeolites

Dirk Mehlhorn,[a] Rustem Valiullin,*[a] Jörg Kärger,[a] Kanghee Cho,[b] and Ryong Ryoo*[b]

Specially synthesized extra-large crystallites of zeolite LTA with intentionally added mesoporosity are used for an in-depth study of guest diffusion in hierarchical nanoporous materials by the pulsed field gradient NMR technique. Using propane as a guest molecule, intracrystalline mass transfer is demonstrated to be adequately described by a single effective diffusivity resulting from the weighted average of the diffusivities in the two (micro- and meso-) pore spaces. Gas-kinetic order-of-magnitude estimates of the diffusivities are in satisfactory agreement with the experimental data and are thus shown to provide a straightforward means for predicting and quantifying the benefit of hierarchically structured nanoporous materials in comparison with their purely microporous equivalent.

1. Introduction

The technological exploitation of nanoporous materials, notably in mass conversion by shape-selective catalysis[1] and mass separation by molecular sieving and selective adsorption,[2] is based on the similarity between the molecular sizes and pore dimensions, which leads to slow diffusion and, hence, the possibility of significant reductions in their performance. Among the various strategies for overcoming such diffusion-related limitations in performance, the generation of mesopores within the microporous bulk phase has attracted particular attention.[3]

However, despite many efforts in the synthesis, characterization, and catalytic assessment of such systems, reports on their diffusion characteristics are still relatively scarce.[4] This is mainly because of the complexity of such systems and the difficulty in generating mesoporous zeolite crystallites large enough to allow the application of microscopic measuring techniques as a prerequisite for an unambiguous determination of intracrystalline diffusivities.[5]

2. Results and Discussion

The primary information provided by pulsed field gradient (PFG) NMR diffusion measurements is contained in the attenuation function $\Psi(g,t)$ of the NMR signal intensity (the spin echo) under the influence of a pair of magnetic field gradient pulses of duration δ, amplitude g, and separation t (the observation time). The gyromagnetic ratio γ is a characteristic constant of the nuclei under consideration ($\gamma_{\text{proton}} \approx 2.67 \times 10^8\ \text{T}^{-1}\,\text{s}^{-1}$). For normal diffusion, that is, for mass transfer in a quasi-continuous medium [Eq. (1)]:[6]

$$\Psi(g,t) = \Psi_0 \exp\{-\gamma^2\delta^2 g^2 D t\} \quad (1)$$

The diffusivity (strictly, the self-diffusivity) D appearing in this equation is defined by the Einstein relation [Eq. (2)]:

$$\langle r^2 \rangle = 6Dt \quad (2)$$

between the mean squared value of the displacements $r(t)$ of the molecules within the sample and the time t during which the displacements are recorded. Alternatively, and completely equivalently, D may be defined by Fick's first law as the factor of proportionality between the flux of labeled molecules, within an entity of unlabeled molecules under uniform overall concentrations, and their concentration gradient.[7]

For ensuring quasi-homogeneity of the diffusion process in mesoporous LTA zeolite crystals, the space scales considered in Equations (1) and (2) must be chosen to notably exceed the diameters of both the micro- and mesopores. In addition, molecular exchange between the micro- and mesopores of the hierarchical zeolites must be implied to be fast in comparison with total observation time.

Figure 1 provides typical examples of the PFG NMR signal attenuation curves observed in our studies. The plots shown in Figure 1a for the purely microporous zeolite are in nice agreement with Equation (1). This reveals the process of normal diffusion in the microporous crystals, which is found to be homogeneous throughout the whole sample. The diffusivities obtained by fitting Equation (1) to the experimental data are shown in Figure 2. A very tiny decrease of the diffusivities with increasing observation time t can be attributed to the onset of restricted diffusion within the individual zeolite crystals. Indeed, using Equation (2) the diffusion path lengths during the observation times studied are found to be of the order of 1 μm for the largest observation times, which can give rise to such tiny effects as those observed.[6]

The plots shown in Figure 1b and c for the mesoporous zeolites reveal two notable differences from the case of the purely

[a] D. Mehlhorn, Dr. R. Valiullin, Prof. Dr. J. Kärger
Faculty of Physics and Earth Science
University of Leipzig
Linnèstr. 5, 04103 Leipzig (Germany)
E-mail: valiullin@uni-leipzig.de

[b] K. Cho, Prof. Dr. R. Ryoo
Center for Functional Nanomaterials
Department of Chemistry and Graduate School of
Nanoscience and Technology (WCU)
KAIST, Daejeon 305-701 (Korea)
E-mail: ryongryoo@kaist.ac.kr

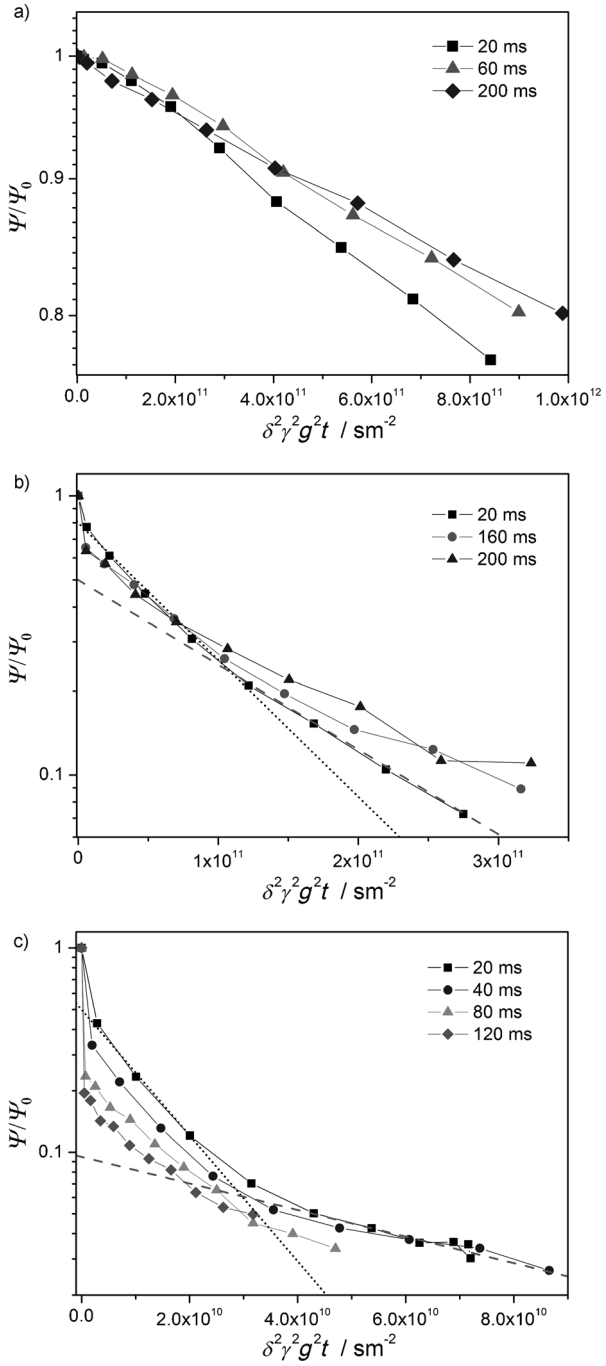

Figure 1. PFG NMR attenuation curves for propane in NaCaA-0 (a), NaCaA-2 (b), and NaCaA-5 (c) for different observation times t measured at 25 °C. The dotted and dashed lines provide an estimate of the mean and the smallest value of the intracrystalline diffusivities, respectively. Note the differences in the scale of the abscissas in (a)–(c), corresponding to the differences in the absolute values of the resulting diffusivities as shown in Figure 2.

microporous sample (Figure 1 a) and the behavior expected on the basis of Equation (1), namely: 1) a first, very steep decay for small $\gamma^2\delta^2g^2t$ values, which increases with increasing observation time and which is much more pronounced in the sample with the larger mesopore volume; and 2) a clear deviation from the exponential shape.

The first peculiarity in the attenuation plots, namely the first steep decay, may be rationalized as the consequence of the increasing diffusivities in the mesopores. This allows more and more molecules to leave the individual crystals with increasing observation times as compared to the microporous analogues. Owing to the high mobility of molecules in the extracrystalline space filled with the gaseous phase, they undergo very large displacements corresponding to extremely high diffusivities which, with Equation (1), are seen to give rise to a first very fast decay in the signal attenuation. This part of the signal attenuation is of no relevance, therefore, for the determination of the intracrystalline diffusivities.

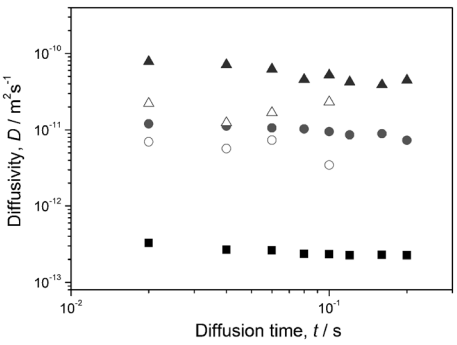

Figure 2. Diffusivities of *n*-propane in NaCaA-0 (squares), -2 (circles), and -5 (triangles) determined from the PFG NMR attenuation curves in Figure 1 a–c. The mean diffusivities are indicated by the full symbols, whereas the open symbols represent the minimum values of the diffusivities.

For an explanation of the second peculiarity we have to take into account that the guest mobility and, hence, the intracrystalline diffusivity in the mesoporous zeolites depends on the relative amount of the mesopores as compared to the overall pore space and on the size of the mesopores. Either of these properties may be expected to vary within a given crystal as well as on considering different crystals. In a sample with varying diffusivities, the overall signal attenuation results as the weighted mean of Equation (1) [Eq. (3)]:

$$\Psi(g,t) = \Psi_0 \int p(D)\exp\{-\gamma^2\delta^2g^2Dt\}\mathrm{d}D \qquad (3)$$

with $p(D)$ denoting the probability (density) that the local diffusivity, as determined by the pore space probed by an arbitrarily selected molecule during the diffusion time, is equal to D. It is further assumed in Equation (3) that different "phases" in the sample with different mobilities are not strongly weighted by their transverse nuclear relaxation rates. The latter condition was as well fulfilled in our experiments performed with the use of extremely large gradient intensities allowing the measurements to be done with very short time intervals (≈2–3 ms in total) in the NMR pulse sequence where the transverse nuclear relaxation occurs.

With Equation (3), application of Equation (1) to the initial slope of the $\ln\Psi$ versus $\gamma^2\delta^2g^2t$ representation (as exemplified by the dotted lines in Figure 1 b and c; note that the very steep decay due to diffusion in the extracrystalline space is excluded from the consideration) is easily seen[6] to provide the

mean value [Eq. (4)]:

$$D_{\text{mean}} = \int Dp(D)\mathrm{d}D \tag{4}$$

of the diffusivities within the sample. Likewise, the slope of the final part of the $\ln\Psi$ versus $\gamma^2\delta^2g^2t$ representation (the dashed lines in Figure 1 b,c) may be used as an estimate of the smallest diffusivities.

Interestingly, the curvature in the $\ln\Psi$ versus $\gamma^2\delta^2g^2t$ representations in Figure 1 b and c does not vary significantly with increasing observation time, thus indicating that the distribution of the diffusivities remains essentially unaffected. With Equation (2) and the diffusivities given in Figure 2, the diffusion path lengths during the largest observation times are found to be of the order of 10 μm, which are seen to approach the crystal sizes. Sample heterogeneities within the individual crystals must therefore be expected to be averaged out with increasing observation time. Hence, sample heterogeneities within the individual crystallites would give rise to a change of the attenuation plots towards a single-exponential decay, in contrast to experimental observation. The distribution $p(D)$ in the diffusivities is most likely caused, therefore, by a variation in the mesopore contents on considering different crystals.

Figure 2 summarizes the diffusivities of propane in the different LTA samples determined from the PFG NMR attenuation plots as exemplified in Figure 1. The mean diffusivities following from the first slope for the mesoporous zeolites (dotted lines) are indicated by full circles (NaCaA-2) and triangles (NaCa-5) and may be directly compared with the diffusivities (full squares) in the purely microporous sample (NaCa-0; the size of the symbols corresponds to the uncertainty of the data). The open symbols are taken from the slope in the last part of the attenuation curves (dashed lines in Figure 1 c). They represent the minimum values of the diffusivities in the mesoporous zeolites as accessible in our diffusion experiments. Although they have to be considered only as estimates (therefore the uncertainty is not shown), in complete agreement with the expected behavior, the difference between the mean and minimum diffusivities—as an expression of the variation in the mesopore space geometry between different crystals—is found to be slightly larger for the sample with the larger content of mesopores.

Most importantly, over the considered interval of observation times, the diffusivities are found to remain essentially constant. Over the space scale (100 nm up to ≈10 μm) and time scale (10 to 200 ms) considered in our experiments, mass transfer is thus demonstrated to follow the laws of ordinary diffusion. For the purely microporous sample, this result is not unexpected. It confirms the results of previous experiments with NaCaA-type zeolites[8] where the intracrystalline diffusivity of propane at room temperature was found to be of the order of $4\times10^{-13}\ \mathrm{m^2\,s^{-1}}$.

The occurrence of ordinary diffusion, however, is not a matter of course for the mesoporous zeolites. It can only be observed under the conditions of fast exchange between the two pore spaces. Therefore, the effective intracrystalline diffusivity in the mesopore space can be assumed to follow the fast-exchange expression of the two-region model of molecular diffusion [Eq. (5)]: [6b,9]

$$D_{\text{eff}} = p_{\text{micro}}D_{\text{micro}} + p_{\text{meso}}D_{\text{meso}} \tag{5}$$

with $p_{\text{micro(meso)}}$ and $D_{\text{micro(meso)}}$ denoting, respectively, the relative number of molecules in the micro- (meso-) pores and their diffusivities.

For an order-of-magnitude estimate, the mesopore system is assumed to consist of straight channels of uniform diameter d to which we apply the Knudsen relation [Eq. (6)]: [6c,10]

$$D_{\text{meso}} = \frac{d}{3}\sqrt{\frac{8RT}{\pi M}} \tag{6}$$

with M denoting the molecular weight of the diffusant. Importantly, the assumption of the channel-like geometry means that the solely mesoporous space is permeable, as has been proven for this type of mesoporous zeolite,[4b] and the diffusion process therein can be characterized by a finite, long-range diffusivity. For an estimate of the relative number of molecules in the mesopores we use Equation (7):

$$p_{\text{meso}} = N_{\text{meso}}/(N_{\text{meso}} + N_{\text{micro}}) \tag{7}$$

where the number N_{meso} of molecules in the mesopores is calculated by the ideal gas equation and the total number $N_{\text{micro}}+N_{\text{meso}}$ of molecules is known from the number of guest molecules that have been introduced into the sample tube.

From the adsorption isotherms presented in the literature,[11] the guest pressure P in equilibrium with the given guest loading of three molecules per large cavity may be set as $P\approx5.3\times10^3$ Pa. The pore diameter d can be estimated from the capillary-condensation pressure in Figure 4 to be about 5 nm. With the resulting values, one finally obtains $p_{\text{meso}}\approx1.0\times10^{-4}$ for NaCaA-2 and $p_{\text{meso}}\approx2.3\times10^{-4}$ for NaCaA-5 and $D_{\text{meso}}\approx6.3\times10^{-7}\ \mathrm{m^2\,s^{-1}}$. With Equation (5), the contributions of the mesopores to the overall intracrystalline diffusivities is thus found to be $p_{\text{meso}}D_{\text{meso}}\approx6.3\times10^{-11}\ \mathrm{m^2\,s^{-1}}$ for NaCaA-2 and $1.5\times10^{-10}\ \mathrm{m^2\,s^{-1}}$ for NaCaA-5. Note that because the mesopore space is in fact tortuous, the estimated $p_{\text{meso}}D_{\text{meso}}$ values give an upper-limit estimate.

3. Conclusions

The experimental diffusivity data and their comparison with the order-of-magnitude estimate based on a simplified gas-kinetic model allow the following conclusions:

1) The presence of mesopores leads to a dramatic enhancement of the intracrystalline diffusivities.
2) Mass transfer is still found to obey the laws of normal diffusion as in the purely microporous ("parent") samples, which indicates fast molecular exchange between the micro- and

mesopore spaces. One has to conclude, therefore, that the overwhelming part of the guest molecules, on their trajectories during uptake and release, alternate between positions in the two pore spaces.

3) Their dramatic enhancement in comparison with the purely microporous zeolites indicates that intracrystalline diffusion in the mesoporous zeolites is exclusively determined by mass transfer through the mesopores.
4) By implying that the mesopore system is formed by straight channels of uniform diameter, an order-of-magnitude estimate of the overall diffusivity leads to values which are in a reasonable agreement with the experimental data. Small differences can be referred to the influence of the tortuosity of the mesopore space and of the pore size variation which, in this rough model, are not taken into consideration. Both these influences are known to lead to an additional decrease in the diffusivity.[12] Their effect decreases with increasing porosity, in complete agreement with our experimental finding.

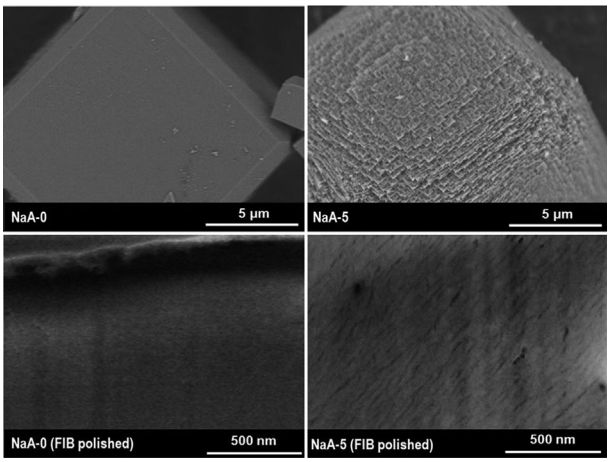

Figure 3. SEM images of non-mesoporous (NaA-0, left column) and mesoporous (NaA-5, right column) LTA zeolite samples: the top images were taken from the external surfaces of calcined samples and the bottom images were taken after cross-sectional polishing by a focused gallium ion beam. The numbers following "NaA-" in the sample name mean the mole percent of organosilane surfactant to entire silica species (silicate + organosilane) in the initial synthetic gel. The dark, slanted lines in the lower right image indicate mesoporous channels exposed at the cross-sectional cut.

Experimental Section

For the synthesis of mesoporous LTA zeolite with crystals of the size required for such studies, we modified our procedure described in ref. [4b]: fumed silica was used as a silica source instead of sodium metasilicate. Triethanolamine was added to the typical gel composition of mesoporous LTA zeolite, as a reagent to increase the crystal size.[13] Three zeolite samples with different mesoporosity levels were synthesized from the gel compositions of 100-*n* SiO_2/333 Na_2O/67.0 Al_2O_3/20 000 H_2O/*n* OSS/*m* triethanolamine, where *n* was 0, 2, or 5. The corresponding number of triethanolamine moles (*m*) was increased to 200, 400, and 666, respectively, to compensate for the crystal size decreasing effect of the amount of organosilane surfactant. Zeolite crystallization was performed under static conditions. The remainder of the synthesis procedure was the same as in ref. [4b]. The role of triethanolamine was to chelate aluminate anions, so that the alumina source could be released very slowly during the crystallization. Under this situation, the generation of zeolite nuclei was known to be suppressed. This led to the generation of large crystals. An overview of the thus-produced series of LTA zeolites with varying contents of mesopores is provided by the SEM images shown in Figure 3. All LTA zeolite samples were calcined at 623 K and ion-exchanged with Ca^{2+}. Calcined samples (1.0 g) were dispersed in 1.0 M $CaCl_2$ aqueous solution, with magnetic stirring for 6 h at room temperature (293 K). This treatment was repeated three times. It was confirmed that the morphology, particle size, and external/internal mesopore structure of all samples were maintained after calcination and ion-exchange treatments.

A summary of the sample data that are of particular relevance for a discussion of the diffusion results is given in Figure 4. The mesoporosity of the LTA zeolite samples, formed by the pores with a diameter of a few nanometers, is seen to gradually increase with the amount of organosilane surfactants, with a mean crystal size of about 11 μm, which remains essentially the same in all samples.

The self-diffusion measurements were performed by means of the PFG NMR technique with the 13-interval stimulated-echo-pulse sequence,[6] thus allowing a variation of the observation time from 10 up to 200 ms. The measurements were performed at room temperature (25 °C) in sealed glass tubes 7 mm in diameter with a filling height of about 10 mm. Propane, with a loading of three molecules per large cavity (α-cage), was used as a probe molecule. With the PFG NMR spectrometer used in these studies,[14] magnetic field gradient pulse amplitudes up to 35 $T m^{-1}$ could be attained. Depending on the measuring conditions, the diffusion path lengths covered in the experiments ranged from about 100 nm up to distances comparable with the crystal sizes. It could, in particular, be ensured that the intracrystalline diffusivities in the purely micropo-

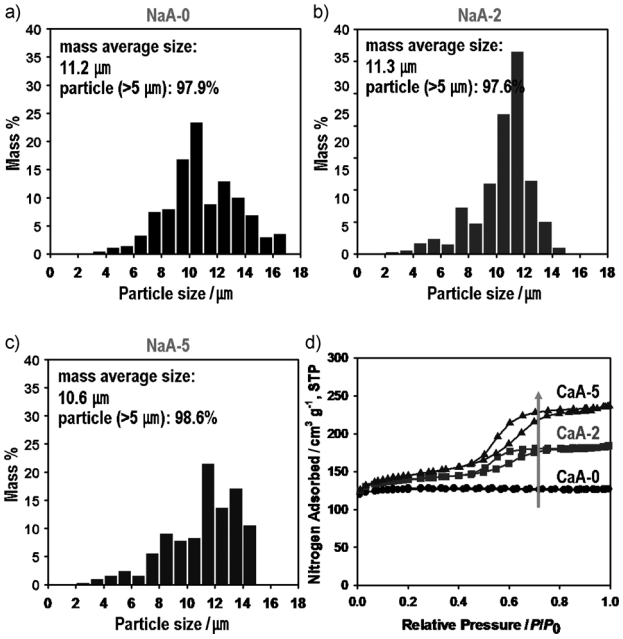

Figure 4. Particle size distribution of three as-synthesized LTA zeolites (a–c) and nitrogen sorption isotherms of their Ca^{2+} forms, CaA-*n* (d). The resulting BET surface area and mesopore volume of CaA-0, -2, and -5 are (422.26, 0.005), (468.53, 0.110), and (491.06 $m^2 g^{-1}$, 0.218 $cm^3 g^{-1}$), respectively.

rous and in the two mesoporous zeolites were determined under identical and, hence, completely comparable measuring conditions.[9a]

Acknowledgements

Financial support by the National Honor Scientist Program of the Ministry of Education, Science and Technology in Korea and the Deutsche Forschungsgemeinschaft in Germany is gratefully acknowledged.

Keywords: intracrystalline diffusion · mass transfer · mesoporous materials · NMR spectroscopy · zeolites

[1] G. Ertl, H. Knözinger, F. Schüth, J. Weitkamp, *Handbook of Heterogeneous Catalysis, 2nd ed.*, Wiley-VCH, Weinheim, **2008**.
[2] F. Schüth, K. S. W. Sing, J. Weitkamp, *Handbook of Porous Solids*, Wiley-VCH, Weinheim, **2002**.
[3] a) W. Fan, M. A. Snyder, S. Kumar, P. S. Lee, W. C. Yoo, A. V. McCormick, R. L. Penn, A. Stein, M. Tsapatsis, *Nat. Mater.* **2008**, *7*, 984 – 991; b) M. Choi, H. S. Cho, R. Srivastava, C. Venkatesan, D. H. Choi, R. Ryoo, *Nat. Mater.* **2006**, *5*, 718 – 723; c) H. Wang, T. J. Pinnavaia, *Angew. Chem.* **2006**, *118*, 7765 – 7768; *Angew. Chem. Int. Ed.* **2006**, *45*, 7603 – 7606; d) D. Verboekend, J. Perez-Ramirez, *Chem. Eur. J.* **2011**, *17*, 1137 – 1147; e) J. Pérez-Ramírez, S. Mitchell, D. Verboekend, M. Milina, N. L. Michels, F. Krumeich, N. Marti, M. Erdmann, *ChemCatChem* **2011**, *3*, 1731 – 1734.
[4] a) J. C. Groen, W. D. Zhu, S. Brouwer, S. J. Huynink, F. Kapteijn, J. A. Moulijn, J. Perez-Ramirez, *J. Am. Chem. Soc.* **2007**, *129*, 355 – 360; b) K. Cho, H. S. Cho, L. C. de Menorval, R. Ryoo, *Chem. Mater.* **2009**, *21*, 5664 – 5673; c) Y. Liu, W. P. Zhang, Z. C. Liu, S. T. Xu, Y. D. Wang, Z. K. Xie, X. W. Han, X. H. Bao, *J. Phys. Chem. C* **2008**, *112*, 15375 – 15381; d) R. Valiullin, J. Kärger, K. Cho, M. Choi, R. Ryoo, *Microporous Mesoporous Mater.* **2011**, *142*, 236 – 244.
[5] a) C. Chmelik, L. Heinke, R. Valiullin, J. Kärger, *Chem. Ing. Tech.* **2010**, *82*, 779 – 804; b) C. Chmelik, J. Kärger, *Chem. Soc. Rev.* **2010**, *39*, 4864 – 4884.
[6] a) P. T. Callaghan, *Principles of Nuclear Magnetic Resonance Microscopy*, Clarendon Press, Oxford, **1991**; b) W. S. Price, *NMR Studies of Translational Motion*, University Press, Cambridge, **2009**; c) M. Dvoyashkin, R. Valiullin, J. Kärger, *Phys. Rev. E* **2007**, *75*, 041202; d) J. Kärger in *Science and Technology—Molecular Sieves, Vol. 7* (Eds.: H. G. Karge, J. Weitkamp), Springer, Berlin, **2008**, pp. 85 – 133.
[7] J. Kärger in *Leipzig, Einstein, Diffusion* (Ed.: J. Kärger), Leipziger Universitätsverlag, Leipzig, **2007**, pp. 1 – 40.
[8] W. Heink, J. Kärger, H. Pfeifer, K. P. Datema, A. K. Nowak, *J. Chem. Soc. Faraday Trans.* **1992**, *88*, 3505 – 3509.
[9] a) R. Valiullin, J. Kärger, *Chem. Ing. Tech.* **2011**, *83*, 166 – 176; b) J. Kärger, H. Pfeifer, W. Heink, *Adv. Magn. Reson.* **1988**, *12*, 2 – 89.
[10] F. Rittig, C. G. Coe, J. M. Zielinski, *J. Phys. Chem. B* **2003**, *107*, 4560 – 4566.
[11] D. M. Ruthven, K. F. Loughlin, *J. Chem. Soc. Faraday Trans. 1* **1972**, *68*, 696 – 708.
[12] C. N. Statterfield, *Mass Transfer in Heterogeneous Catalysis*, MIT Press, Cambridge, MA, **1970**.
[13] G. Scott, R. W. Thompson, A. G. Dixon, A. Sacco, *Zeolites* **1990**, *10*, 44 – 50.
[14] a) P. Galvosas, F. Stallmach, G. Seiffert, J. Kärger, U. Kaess, G. Majer, *J. Magn. Reson.* **2001**, *151*, 260 – 268; b) F. Stallmach, P. Galvosas, in *Annual Reports on NMR Spectroscopy, Vol. 61* (Ed.: G. A. Webb), Academic Press, San Diego, **2007**, pp. 51 – 131.

Received: January 18, 2012
Published online on March 2, 2012

